

FAST LOG-GABOR-BASED NONLOCAL MEANS IMAGE DENOISING METHODS

Song Zhang and Huajiong Jing

Hangzhou Dianzi University, China

ABSTRACT

This paper explores the possibility of incorporating log-Gabor features into nonlocal means image denoising framework. It is found that log-Gabor features are better choice for this task than previously studied geometrical features. Moreover, we combine log-Gabor features with original image patch information to arrive at mixed similarity measure, which leads to further denoising performance improvement. In addition, we test a random projection-based approach to nonlocal means speed-up, guided by the well-known Johnson-Lindenstrauss lemma. Experimental results are quite encouraging.

Index Terms— Nonlocal means, log-Gabor features, mixed similarity measure, dimensionality reduction, Johnson-Lindenstrauss lemma

1. INTRODUCTION

In this paper, we focus on typical image denoising problem formulated as

$$y(i) = x(i) + n(i), \quad (1)$$

where x and y are the original and corrupted images respectively, and n is AWGN process with variance of σ^2 . The goal is to restore x from y .

Most of modern adaptive filtering approaches [1] to image denoising take the following form:

$$\hat{x}(i) = \frac{\sum_j w_{ij} y(j)}{\sum_j w_{ij}}, \quad (2)$$

where the mechanisms for computing weights w_{ij} 's determine the types of concrete denoising algorithms and their performances.

Imagine the virtual oracle scenario, where we have precise knowledge of the original image. Given this assumption, the optimal weights can in principle be obtained by optimizing the bias-variance trade-off resulting from the corresponding filtering operations. Although the derived expressions may still be very complicated, intuitively the correct weight w_{ij} should be approximately decreasing function of the difference $|x_i - x_j|$ between pixels i and j . The observations made above are easily understood by considering the extreme noise-free case, where the optimal weight $w_{ij} = 1$ if $x_i = x_j$ and $w_{ij} = 0$ otherwise (under

the condition that there exist pixels with their intensities equal to that of pixel i).

However, the original image is simply unavailable. Even more importantly the noise makes it rather difficult to directly estimate the similarity (or dissimilarity) between pixels. Buades [2] proposed nonlocal means (NLM) solutions to these problems by estimating pixel similarity based on patch information around the associated center pixels. Specifically, in NLM the filtering weights w_{ij} 's are computed as

$$w_{ij} = K(-D(P_i, P_j)), \quad (3)$$

where $K(\cdot)$ is the kernel function and $D(P_i, P_j)$ measures the similarity (or dissimilarity) between two patches surrounding pixels i and j , say Euclidian difference between them.

The rationale behind the patch computation in NLM can be easily seen if we assume that the original image is piece-wise constant and the patches are completely contained within one uniform region, where the patch operation is perfect means to reduce the noise effect and yield much more accurate similarity estimates than its pixel-wise counterpart. Nevertheless, for more complicated image models it becomes uncertain whether such patch-based estimates are optimal. In fact, there have been some works to generalize NLM weights definition (3) to

$$w_{ij} = K(-D(F_i, F_j)), \quad (4)$$

where F_i and F_j are feature vectors extracted from local neighborhoods corresponding to pixels i and j . Ji et al. [3] introduced the Zernike moments into NLM filter and reported improved denoising performance than the original NLM filter. Grewenig et al. [4] studied systematically rotationally invariant similarity measures for NLM based on geometric moments including Hu moments and Zernike moments. Wang et al. [5] proposed Gabor features-based NLM denoising scheme, yet solely aimed at purely textured images.

Inspired by these works, the current paper explores the possibility of incorporating log-Gabor features into NLM image denoising, more specifically estimating pixel similarity by comparing associated local log-Gabor feature vectors. It is found that these kind of geometric features perform better for NLM denoising than those previous studied. Furthermore, we combine the log-Gabor features with image patch information to obtain mixed similarity measures, resulting in more powerful adaptivity to local

image characteristics and in turn additional denoising performance boost.

On the other hand, lifting to higher dimensional feature space for better similarity estimates is by no means free lunch. The curse of dimensionality is just the cost to pay. There have been much efforts made to reduce the complexity of NLM while incurring little performance loss. This paper studies a random projection-based approach to NLM speed-up and tests extensively the resulting complexity-performance trade-offs. Experiments results show that the acceleration scheme can achieve a net 3-fold speed-up with negligible PSNR loss.

The rest of the paper is structured as follows. Section 2 first highlights the advantages of log-Gabor features with respect to Gabor features. Next the pipeline of log-Gabor-based NLM denoising algorithm is described, after which we introduce the mixed similarity and filtering weights. Section 3 explains the principles of random projection-based NLM acceleration. We give experiment results in Section 4 to prove the effectiveness of the proposed modifications. Finally, Section 5 draws conclusions.

2. LOG-GABOR-BASED NLM DENOISING

2.1. Log-Gabor vs. Gabor Features

As the most widely-used image analysis tool, Gabor features are produced by a multi-scale and multi-orientation filter bank with parametric frequency response as follows:

$$G(u, v) = \exp\left(-\frac{(u - u_0)^2 + (v - v_0)^2}{\sigma^2}\right), \quad (5)$$

where (u_0, v_0) is center frequency and σ determines filter bandwidth. Despite its theoretically optimal joint spatial-frequency localization capability, Gabor filter bank is not flawless. In practice, to prevent strong interference of DC component with feature extraction, the associated filters are required to have sufficient DC suppression, which limits the maximal attainable bandwidth of Gabor filters (about 1 octave) and in turn the high-frequency coverage efficiency of Gabor filter bank.

Field [6] introduced simple logarithms into frequency response to arrive at log-Gabor filter bank with parametric response modified as

$$LG(f, \theta) = \exp\left(-\frac{[\log(f/f_0)]^2}{\sigma_f^2}\right) \exp\left(-\frac{(\theta - \theta_0)^2}{\sigma_\theta^2}\right), \quad (6)$$

where (f, θ) is polar frequency description, (f_0, θ_0) is center frequency, while σ_f^2 and σ_θ^2 denote the bandwidths in radius and angle respectively. It is easily seen that log-Gabor filters have perfect DC suppression (vanishing response) and much better high-frequency characterization capability than their Gabor counterparts. In addition, the tailing behaviors of log-Gabor filters are closer to $1/f$ law dominating natural images than Gabor filters.

2.2. Log-Gabor-Based NLM Denoising Scheme

The steps of the proposed log-Gabor-based denoising scheme follow essentially those of [5] with some modifications. After application of log-Gabor filter bank to input image, we obtain M feature maps, or at each pixel location there is an M -dimensional feature vector, where M is the number of filter bank members. To reduce the impact of noise on feature extraction accuracy, low-pass filtering with minimal spatial support (i.e. minimal high-frequency loss) is performed on each feature image. Specifically [5],

$$\mathbf{v}_k = \mathbf{g}_\rho * \mathbf{z}_k, \quad (7)$$

where \mathbf{z}_k is the original k th feature image and \mathbf{g}_ρ is Gaussian filter with spatial support size ρ .

Due to different output ranges from different feature maps, normalization is necessary for correct estimation of pixel similarity based on log-Gabor feature vectors. In this paper, we normalize the corrected feature maps \mathbf{v} 's to the range of input noisy image, that is

$$F_k(i) = \frac{v_k(i) - \min_i v_k(i)}{\max_i v_k(i) - \min_i v_k(i)}. \quad (8)$$

Finally, the filtering weights are computed by instantiating (3) as

$$w_{ij} = \exp\left(-\frac{D_F(i, j)}{h_{LG}^2}\right), \quad (9)$$

where h_{LG} is smoothing constant and the similarity (or dissimilarity) between pixels i and j is computed as

$$D_F(i, j) = \frac{\sum_k (F_k(i) - F_k(j))^2}{M}. \quad (10)$$

2.3. Mixed Similarity and Weight

It is found that the new log-Gabor-based NLM algorithm performs quite well for denoising most of natural images, yet not so for denoising images with relatively strong regular texture structures. Image patch information is believed to be more suitable for similarity estimation among such repetitive patterns. Therefore, we combine the log-Gabor features with patch information to arrive at the following mixed similarity and weights:

$$w_{ij} = \exp\left(-\frac{1}{2} \left[\frac{D_F(i, j)}{h_{LG}^2} + \frac{D_P(i, j)}{h_P^2} \right]\right), \quad (11)$$

where $D_P(i, j)$ is a kind of distance, say mean squared difference or windowed squared difference, between patches surrounding pixels i and j respectively, and h_P is the corresponding smoothing constant. Such combination may be thought of a new level of lifting for flattening image local manifolds, and has interesting connection with previous works such as iconic feature-based image registration [7] and attribute distance weighted average-based denoising [8].

3. RANDOM PROJECTION FOR NLM SPEED-UP

The most natural approach to removing curse of dimensionality is to project the original data onto an informative low-dimensional space. Besides, such operation tends to produce improved performances [9], since most of high-dimensional data actually live in low-dimensional manifolds. However, typical ways to mine the internal low-dimensional structures, say PCA or its nonlinear version, are themselves a little bit time-consuming, which may cancel to some extent the benefits they bring in terms of speed.

There does exist another attractive solution, that is, by random projection. Johnson and Lindenstrauss [10] first proved the following seminal lemma:

Lemma: Assume $0 < \varepsilon < 1$ and a collection S composed of n points in R^d . If $k \geq k_0 = O(\varepsilon^{-2} \log n)$, there exists a linear mapping f from R^d to R^k , such that for any $u, v \in S$

$$(1 - \varepsilon)\|u - v\|^2 < \|f(u) - f(v)\|^2 < (1 + \varepsilon)\|u - v\|^2. \quad (12)$$

Moreover, the linear mapping guaranteed by the lemma can be readily realized as random projection, a consequence of the law of large numbers. Unlike PCA-like dimensionality reduction methods, the construction of random projection matrix is almost effortless, which is desirable for massive data processing problems, such as searching and distance computation.

The complexity analysis of random projection-based NLM is immediately available. Given N pixels of input image, we estimate the similarity between two pixels by computing distance between two corresponding M -dimensional feature vectors. Consider the more practical semi-nonlocal filtering paradigm of NLM, i.e. confining the filtering range to neighborhood of size L . Thus the complexity of direct implementation of NLM is $O(NML)$. On the other hand, given the random projection matrix, the complexity of projecting all N M -dimensional feature vectors onto lower-dimensional R^k is $O(NMK)$, while that of post-dimensionality-reduction NLM computation becomes $O(NLK)$. As noted before, the complexity of the construction of random projection matrix is negligible compared with that of projection and similarity evaluation. In summary, the acceleration ratio is about $ML/(MK+KL)$. For typical parameter values adopted in the experiment, $M = 60$, $K = 20$, $L = 200$, these amount to more than 2-fold speed-up.

Despite the theoretical guarantee, the applicability of the asymptotic results to similarity computation and denoising remains to be studied. In fact, this paper is not the first attempt to incorporate random projection into NLM. Lai et al. [11] proposed the random projection-based approach to NLM acceleration, yet only for baseline NLM. Besides, the results reported in [11] are rather limited. We extend the idea to general geometrical feature-based NLM, and perform extensive experiments on the complexity-performance trade-off and the impact of the type of random

Table 1. Denoising results (PSNR, in dB) comparison between the proposed schemes (the last 2 columns) and several other geometrical features-based NLM algorithms including baseline NLM. Noise intensity $\sigma = 20$, and each figure is the average of those corresponding to 5 independent noise realizations.

	Buades [2]	Ji [3]	Grewenig [4]	Wang [5]	log-Gabor	Mixed
Barbara	29.80	27.29	25.60	24.72	27.51	30.02
Bridge	25.81	24.84	24.66	24.04	26.24	26.48
CMan	29.33	27.67	24.92	25.28	29.24	29.69
Couple	28.78	28.9	27.37	24.47	29.63	29.86
Hill	27.40	26.79	26.80	24.22	27.76	28.20
Lema	31.24	31.3	30.50	24.34	32.01	32.40
Man	29.23	28.93	28.40	25.17	29.96	30.22
Peppers	29.23	29.38	28.7	25.72	30.55	30.83

projection on denoising performances. Therefore, the current work is still believed to be meaningful and constitute complement to [11].

4. EXPERIMENTAL RESULTS

The parameter settings for log-Gabor-based NLM are as follows. There are 10 scales in log-Gabor filter bank, with the maximal frequency and the ratio between neighboring frequencies to be 0.5 and 2 respectively. Meanwhile, we set 6 different orientations $\{0, \pi/6, \pi/3, \pi/2, 2\pi/3, 5\pi/6\}$, thus combined with scale settings leading to 60-dimensional feature vector associated with each pixel. Bandwidth constants $\sigma_f = \log_e 0.55$ and $\sigma_\theta = \pi/7.2$, while smoothing constants $h_{LG} = 0.5\sigma$ and $h_p = \sigma$, where σ is noise standard deviation. Filtering window is set to be 13×13 . The results of the proposed method are compared with those of baseline NLM [2], Zernike moments-based NLM [3], Hu moments-based NLM [4] and Gabor-based NLM [5], which are implemented strictly as specified in the original papers or with codes shared by the authors.

4.1. Denoising Performances Comparison

We have carried out denoising experiments on different natural images across a wide range of noise levels. Due to limit of space, only results under typical noise intensity ($\sigma = 20$) are shown, with similar phenomena observed for other noise levels.

The superiority of log-Gabor NLM for denoising most of test images with respect to baseline NLM and other geometrical feature-based NLM is clearly seen from Table 1. However, for images with more regular texture structures such as Barbara, the log-Gabor-based NLM does not perform quite well. After combination of log-Gabor features with patch information, the resulting mixed similarity-based NLM achieves even better denoising performances, with significant boost for images like Barbara, where log-Gabor-based NLM fails.

4.2. Tests on Random Project-based Speed-up for NLM

Table 2. Performance-complexity trade-offs by random projection method 1 under noise level $\sigma = 20$. Each figure is generated by averaging results corresponding 5 independent random matrix realizations. The column with header “60” amounts to no random projection.

	60	50	40	30	20	10
Barbara	27.51	27.53	27.53	27.56	27.25	26.98
Bridge	26.23	26.22	26.18	26.15	26.02	25.70
CMan	29.17	29.11	29.11	29.05	28.92	28.63
Couple	29.63	29.57	29.50	29.49	29.38	28.99
Hill	27.77	27.76	27.72	27.70	27.63	27.20
Lema	32.01	31.93	31.90	31.77	31.67	31.17
Man	29.96	30.01	30.01	29.93	29.86	29.40
Peppers	30.64	30.59	30.54	30.49	30.32	29.85

There are several different methods to construct random projection matrix. While they have similar asymptotic performance guarantees, the practical difference between them when incorporated into NLM framework remains to be studied. We choose 6 random matrix construction methods. Method 1 corresponds to that used for constructive proof of J-L lemma [10]. This also amounts to normal orthogonal version of Gaussian matrix (with components generated by i.i.d. standard Gaussian distribution, termed method 2). Method 3 and method 4 are proposed in [12] for more convenient construction. The distribution underlying Method 3 give equal probability to 1 and -1 , while that of method 4 assigns greater probability to 0, making the constructed matrix very sparse, which is desirable for fast matrix-vector multiplication computation. Method 5 and method 6 are the normal and orthogonal counterparts of method 3 and method 4 respectively.

We first test the performance-complexity trade-off associated with random projection, i.e. the impact of the reduced dimensionality on denoising performance. In this paper, random projection is applied to log-Gabor feature vectors to verify its effectiveness. Again due to length limit, only results corresponding to a typical noise level and projection matrix construction method combination are shown. From Table 2, it is observed that reduction of dimensionality from 60 to 20 only incurs 0.2-0.3 dB loss in PSNR, while further dimensionality reduction may cause significant decrease in performance. While these confirm the feasibility of random projection-based acceleration scheme, it should be noted that the phenomena observed here are rather different with those in [11].

We also study the impact of the type of projection matrix construction method on the denoising performance. Fig. 1 gives typical results. It is seen that the normal and orthogonal versions perform slightly better than their plain counterparts, yet with additional cost associated with normalization and orthogonalization.

5. CONCLUSIONS

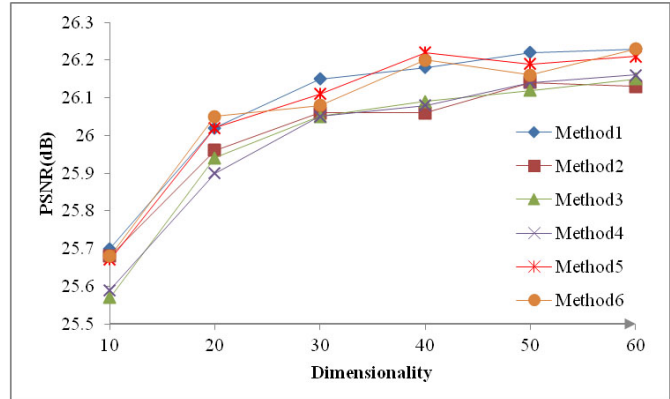


Fig. 1. The impact of the type of random projection method on denoising performance for test image “Bridge” under noise level $\sigma = 20$.

In this paper, we incorporate log-Gabor features into NLM framework for improved denoising performance. Further combination of log-Gabor features with patch information leads to mixed similarity and in turn to additional performance lift. We also study and test extensively the random projection-based NLM speed-up schemes, including quantitative analysis of performance-complexity trade-off and the impact of random projection method on denoising results.

Some future works are in sight. Combination of more meaningful features is believed to yield more powerful similarity estimates, in the spirit of [9]. On the other hand, while the results of the current paper are much more informative than those of [11], more efforts are needed to design practical random projection-based NLM denoising scheme.

6. ACKNOWLEDGEMENT

This work has been supported in part by Zhejiang Provincial Key Laboratory of Technology on Data’s Storage, Transmission and Security (HDU). The partial support from National Natural Science Fund for the Youth of China (41301439) is also gratefully acknowledged.

7. REFERENCES

- [1] P. Milanfar, “A tour of modern image filtering,” *IEEE Signal Processing Magazine*, vol. 30, no. 1, pp. 106 -128, Jan. 2013.
- [2] A. Buades, B. Coll and J. Morel, “A non-local algorithm for image denoising,” *IEEE Computer Society Conference on Computer Vision and Pattern Recognition*, 2005, vol.2, pp. 60-65.
- [3] Z. Ji, Q. Chen and Q. Sun, “A moment-based nonlocal-means algorithm for image denoising,” *Information Processing Letters*, vol. 109, no. 23, pp. 1238-12448, 2009.
- [4] S. Grewenig, S. Zimmer and J. Weickert, “Rotationally invariant similarity measures for nonlocal image denoising,”

Journal of Visual Communication and Image Representation, vol. 22, no. 2, pp. 117-130, 2011.

[5] S. Wang, Y. Xia, Q. Liu, J. Luo, Y. Zhu and D. D. Feng, "Gabor feature based nonlocal means filter for textured image denoising," *Journal of Visual Communication and Image Representation*, vol. 23, no. 7, pp. 1008-1018, 2012.

[6] D. J. Field, "Relations between the statistics of natural images and the response properties of cortical cells," *J. Opt. Soc. Am. A*, vol. 4, no. 12, pp. 2379-2394, 1987..

[7] P. Cachier, E. Bardinet, D. Dormont, X. Pennec and N. Ayache, "Iconic feature based nonrigid registration: the PASHA algorithm," *Computer vision and image understanding*, vol. 89, no.2, pp. 272-298, 2003.

[8] G. Xiong and T. Ding, "ADWA: A filtering paradigm for signal's noise removal and feature preservation," *Signal Processing*, vol. 93, no. 5, pp. 1172-1191, 2012.

[9] D. Van De Ville and M. Kocher, "Nonlocal means with dimensionality reduction and SURE-based parameter selection," *IEEE Transactions on Image Processing*, vol.20, no.9, pp. 2683-2690, Oct. 2011.

[10] W. B. Johnson and J. Lindenstrauss, "Extensions of Lipschitz mappings into a Hilbert space," *Contemporary Mathematics*, vol. 26, pp. 189-206, 1984.

[11] R. Lai and Y. T. Yang, "Accelerating non-local means algorithm with random projection," *Electronics Letters*, vol.47, no.3, pp. 182-183, 2011.

[12] D. Achlioptas, "Database-friendly random projections: Johnson-Lindenstrauss with binary coins," *Journal of computer and System Sciences*, vol. 66, no. 4, pp. 671-687, 2003.